Title: A continuum of CD4+ T cell "help" defines Memory B cell fate

One Sentence Summary: A hierarchy of T-B interactions leads to the generation of functionally distinct memory B cell populations.

Authors: Gretchen Harms Pritchard, Akshay T. Krishnamurty, Lauren Rodda, Courtney McDougal, Laila Shehata, Marion Pepper*

Affiliations: Department of Immunology, University of Washington School of Medicine, Seattle, WA, 98109; USA; *lead contact

Correspondence: mpepper@uw.edu

Abstract:

Humoral immunity depends upon long-lived, antibody-secreting plasma cells and memory B cells (MBCs). MBCs exhibit significant phenotypic and functional heterogeneity. Upon homologous rechallenge, memory B cells thought to be of germinal center (GC) origin rapidly form antibody secreting plasmablasts but rarely enter a new GC, while other, less differentiated memory B cells enter secondary GCs, but do not form plasmablasts. These two populations therefore respond to a subsequent infection by generating antibody-secreting cells to epitopes not recognized by pre-existing serum and new populations of GC-derived MBCs that protect against novel variants. Understanding the mechanisms that regulate the differentiation of each unique population of MBCs during infection will help to define how to optimally drive the formation of these heterogeneous MBC cells via vaccination. We demonstrate a hierarchy of T-B interactions that leads to the generation of functionally distinct memory populations.

Keywords: Humoral immunity, Memory B cell, Malaria, BCL6, S1PR2, Germinal Center, Somatic Hypermutation

Main text:

INTRODUCTION

The generation of effective humoral immunity is the foundation of most successful vaccine strategies (*1*). Humoral immunity is mediated by long-lived plasma cells (LLPCs) and memory B cells (MBCs) activated through their B cell receptors in response to exposure to their cognate antigens (*1, 2*). While pre-existing antibodies secreted by LLPCs can provide immediate defense against invading pathogens, MBCs maintain their BCR expression, and are poised to differentiate into antibody-secreting cells upon secondary antigen encounter (*3*). Yet viruses evolve and therefore so must memory populations to protect against novel epitopes. Understanding the signals that lead to the differentiation of memory B cells with different functional potential will inform optimal vaccine design to protect against infection.

Several studies have revealed that both phenotypically, functionally, and epigenetically diverse MBC populations can form in response to immunization or infection in mice and humans (*4-11*). Using a murine model of malaria infection, we have previously shown that several phenotypically and functionally distinct populations of MBCs arise. IgM+ MBCs that express molecules associated with GC experience (CD80+ CD73+, called Double Positive or DP) are the first to differentiate into antibody secreting cells after a secondary infection. DP CD80+CD73+ swIg+ MBCs form plasmablasts that secrete high concentrations of IgG antibody shortly thereafter while CD80-CD73- Double Negative (or DN) IgD+ MBCs are more naïve-like and thought to predominantly contribute to a subsequent GC response (*5, 9, 11-13*). We therefore sought to understand how each of these MBC subsets forms in the same infectious setting.

The current paradigm regarding the formation of memory B cells suggests that activated B cells undergo iterative interactions with CD4+ T cells which influence their fate, but the details remain unclear. CD4+ T cells and B cells first physically engage at the T-B border and interfollicular regions of the secondary lymphoid organs. CXCR5-expressing T follicular helper (Tfh) cells and CCR7-

expressing B cells can interact through diverse receptor-ligand interactions and the transfer of cytokines and growth factors (*14*). Some activated B cells continue to interact with CD4+ Tfh cells in the GC (GC Tfh) where BCR somatic hypermutation and testing by CD4+ T cells leads to affinity maturation and the eventual exit of diversified MBC and LLPC populations (*15*). Despite years of interrogation, many questions remain about the distinct signals that lead to the differentiation of specific MBC populations.

It has been proposed that DN IgD+ cells arise within days of immunization, express lower affinity, unmutated BCRs and form in a BCL6- and GC-independent manner (*7, 16-22*). More recently Nussenzweig and colleagues described a population of IgD+ memory cells that expressed CD95, GL7, and S1PR2 (associated with GC entry) (*23 figure S1*), suggesting further investigation is needed. DP cells are thought to form in the GC as they can express high affinity, somatically hypermutated BCRs suggestive of GC-residency (*5, 9*). We therefore hypothesized that while the DN IgD+ MBCs are GC-independent, perhaps the DP IgG+ and IgM+ MBCs are GC-dependent.

We used various knockout and reporter mice to test how specific CD4+ T cell interactions and transcriptional programs can influence MBC fate, using the deep knowledge of the DP IgG+ cells to guide our assays. Our results demonstrate that DN IgD+ MBCs do not require cognate interactions with CD4+ T cells, BCL6 or a GC. DP IgM+ MBCs depend upon B cell-intrinsic expression of the GC B cell lineage-defining transcription factor BCL6 but can form in the absence of a GC. Surprisingly, despite not entering the GC, the DP IgM+ MBCs that respond to secondary challenge are traced for S1PR2 expression, suggesting that SIPR2 reports cells fated to form plasmablasts in a secondary response, regardless of their GC-residency. Together, these studies define a hierarchy of T-B interactions that drive the differentiation of functionally distinct MBC populations.

RESULTS

CD4 T cell cognate interactions are required for development of CD73+ MBC populations

We first focused on understanding what types of CD4+ T and B cell interactions were required for the generation of each MBC subset. Previous studies have shown that costimulation through CD40 signaling is insufficient to induce upregulation of CD73 on B cells (*19*). CD4+ T cells and B cells can also interact through cognate interactions, in which a B cell presents peptide:MHC complexes to a CD4+ T cell specific for the same antigen, as well as non-cognate interactions via receptor-ligand pairs. Cognate interactions can induce T cell cytokine production (*24*), alter migration patterns (*25*), and lead to the GC response (*26*). We sought to determine whether MHCII cognate interactions were required for the development of CD73+ MBCs. To do so, we utilized a mixed bone marrow chimeric system using bone marrow from congenically disparate WT and MHC class II transactivator (MHCII) -deficient donor mice transferred into irradiated WT hosts. This system allowed us to compare memory formation in B cells that can make cognate interactions to memory formation in those that cannot in the same inflammatory environment. Reconstituted chimeric mice were infected with *Plasmodium* and the quantity and quality of the MSP1-specific B cell responses were assessed at various time points thereafter. As early as 8 days after infection, there were nearly 10 times more MSP1-specific WT B cells than MHCII-deficient B cells (Fig. 1A). The extent of this defect was greatest 28 days after infection when the WT MSP1-specific B cells were approximately 200 times more abundant than their MHCII-deficient counterparts (Fig. 1A). While there continued to be fewer MHCII-deficient MSP1-specific B cells ~100 days post infection, the defect was less severe than at earlier timepoints (Fig. 1A).

We next examined phenotypic differences of the B cells from the MHC II sufficient and deficient compartments. At day 28 post-infection when the magnitude of the differences in number of cells was the greatest, the majority of the WT cells are in the GC, yet this population is absent in the MHCII-deficient B cells as expected (Fig. S1A) (*27, 28*). We also examined the MBCs at each of the

selected timepoints. While the total IgD+ MBC population was intact at all timepoints, both the IgM+ and swIg+ MHCII-deficient MBC populations were significantly reduced, demonstrating differences in the dependence upon cognate interactions among the MBC isotypes (Figs. 1C, S1B and data not shown). Furthermore, the frequency and number of CD73+ MBCs was reduced in all three MHCII-deficient MBC populations compared to WT MBCs, yet this is such a small portion of the IgD+ (~2%) population that it does not significantly affect the total MSP-specific IgD+ pool (Fig. 1C and 1D). Taken together, these data indicate that cognate interactions with CD4+ T cells are required for the generation and phenotype of CD73+ IgM+ and swIg+, yet the majority of IgD+ MBCs develop in a cognate interaction-independent manner. These data also confirm the stability of the IgD+ MBCs that emerge in this setting, which also helps to explain the partial recovery of the WT:KO B cell ratio at late timepoints.

BCL6 is expressed in early activated B cells

We next sought to dissect the role of the GC in the development of the MBC populations. To do this, we first confirmed that BCL6 is expressed during *Plasmodium* infection with similar characteristics as has been shown in immunization settings. While BCL6 is highly expressed in GC B cells, elegant studies by Okada and colleagues using immunofluorescent microscopy of BCL6-YFP reporting B cells demonstrated that antigen-activated B cells initially up-regulate BCL6 in a T cell-dependent manner in the outer region of the follicle, before the GC has formed (*29*). Moreover, studies from the Haberman laboratory identified perifollicular activated cells that express intermediate levels of BCL6 along with IRF4, and demonstrated that the cells that further upregulate BCL6 enter the GC whereas the cells that further upregulate IRF4 do not (*30*). We therefore sought to better understand the kinetics of BCL6 expression after infection, after excluding plasmablasts (CD138+ cells) from our analysis. In naïve mice and within the first 4 days of *Plasmodium* infection, MSP1-specific cells retained a naïve-like phenotype and did not express BCL6 (Fig. 2A, B). However,

by day 6 post-infection, cells expressing BCL6 began to accumulate and this population was maintained over the timecourse studied. Interestingly, and in contrast to recent studies by Nussenzweig and colleagues in a murine model of vaccination, IgD+ cells do not express BCL6 at any timepoint in our analysis (Fig 2C). At day 6 post infection, the majority of the BCL6 expressing cells were IgM+ cells. However, over time, the proportion of swIg+ cells increased and by day 20 the BCL6+ cells were almost exclusively class-switched. These data are consistent with the immunization studies from Okada and Haberman and indicate that BCL6 is expressed early after activation during infection with *Plasmodium* (*29, 30*). We were not able to detect BCL6+CD80+ cells at any timepoint examined (Fig 2E and data not shown)(Shehata et al. *In press*), consistent with studies showing that BCL6 binds to the CD80 promotor, directly suppressing its expression (*31*).

B cell-intrinsic BCL6 expression is required for the development of *Plasmodium*-specific DP MBCs

To test the requirement of BCL6 for the development of DP MBC populations, we next set up a system in which we could genetically ablate BCL6 in B cells (*32-34*). To accomplish this, we generated B cell conditional BCL6 knock-out (BCL6BKO) mice by crossing *MB1-Cre*+ mice to *Bcl6flx/flx* animals (*35, 36*). Mixed bone marrow chimeric mice were generated with bone marrow from congenically disparate WT and *MB1-Cre*+ *Bcl6flx/flx* (BCL6BKO) animals transferred into sublethally irradiated hosts in order to create an environment in which BCL6-sufficient and -deficient B cells could respond to infection in competition in the same inflammatory environment. After infection with *Plasmodium*, MSP1-specific BCL6BKO did not form GC B cells as expected (*19*), and as seen in their WT counterparts at day 12 or any other time point examined (Fig S2A and data not shown), confirming the important role for BCL6 in GC generation. Next, we determined how the lack of GC B cells among the BCL6BKO B cells impacted the numbers and composition of MSP1-specific MBC populations at subsequent time

points. Mixed WT:BCL6BKO chimeras were infected and MSP1-specific B cells were examined at memory timepoints ≥44 days post-infection. It was immediately evident that the total number of MSP1-specific B cells was reduced in the BCL6BKO B cell population compared to WT B cells in the same animals (Fig S2B).

Among the MBC populations, BCL6 deficiency resulted in a loss of the IgM+ MBCs and swIg+ MBCs (reduced by ~70 and ~97%, respectively), compared to WT MSP1-specific MBCs (Fig. 3A). Analysis of the expression of CD73 and CD80 on each subset further revealed a selective loss of the DP cells that accounted for a significant portion of the IgM+ and swIg+ MBCs that were lacking in the BCL6BKO population (Fig. 3B). BCL6 is therefore critical for the formation of DP MBCs and its ablation has profound effects on MBC populations that have higher frequencies of DP expressing cells (IgM+ and swIg+ MBCs).

BCL6-dependent DP MBCs are required for rapid plasmablast formation

While the preceding data demonstrated that BCL6-deficient B cells do not form DP MBCs, it was possible that we had only altered the phenotype of the MBCs, but not their function. For example, BCL6 can negatively regulate the expression of several molecules associated with the MBC phenotype including CD80 and PD-L2 (*31, 37*). Alternatively, it was also possible that DP MBCs (the major population deleted in the absence of B cell-intrinsic BCL6), were not the only source of novel antibody secreting B220+CD138+ plasmablasts (*5*). Thus, we compared functional responsiveness to rechallenge in the presence or absence of B cell-intrinsic BCL6 expression. WT:BCL6BKO bone marrow chimeric mice were infected, allowed to form memory and subsequently rechallenged with *Plasmodium* at similar memory timepoints that we had previously seen functional plasmablast responses to rechallenge (*5*). As expected, prior to rechallenge, WT B cells consisted of two populations of memory cells: B220+CD138- MBCs and B220^{low}CD138+ LLPCs. LLPCs did not form in the BCL6BKO population as expected based on their GC-dependence (Fig. 3C) (*7*). Similar to our previous

results, WT cells formed an expanded B220+CD138+ plasmablast population and an expanded LLPC population 3 days after rechallenge (Fig. 3C) (*5*). Yet both populations were absent in the BCL6BKO cells by both frequency and number (Fig. 2C). B cell-intrinsic expression of BCL6 is therefore required for the formation of DP MBCs and long-lived plasma cells, and in the absence of these populations, no plasmablasts are produced shortly after rechallenge with *Plasmodium*, again highlighting the importance of the DP MBC populations in a secondary response to infection.

S1PR2 expression history of DP MBC populations

While our data suggested that the BCL6BKO cells were not functional because they could not form GC B cells, there was the distinct possibility that perhaps these cells required BCL6 expression in a GC-independent manner. Indeed, in addition to its myriad functions described above, BCL6 regulates B cell localization through repression of EBI-2, and regulates additional co-stimulatory molecule expression and protection from DNA-damage induced apoptosis (*25, 38, 39*). Therefore, we next decided to use an approach in which we marked the cells that had transited through a GC using a fate reporter. S1PR2 is a migration inhibitory receptor that repels cells away from S1P and thus its expression confines cells within the GC (*40*). S1PR2 expression has been previously used to fatemap GC B cells (*13, 41, 42*). In these mice, ERT2Cre is inserted into exon 2 of the *s1pr2* locus (*S1pr2*-ERT2cre mice) which are then crossed to mice expressing either tdTomato or Zsgreen with a *lox*P-flanked stop cassette (*41*). Upon tamoxifen treatment, cells expressing S1PR2 also express the fluorescent marker, which remains expressed within these cells even after cessation of S1PR2 expression. S1PR2 fate reporter mice were infected with *Plasmodium* and tamoxifen administration was initiated prior to infection and continued throughout the duration of the experiment. To confirm the fidelity of the reporter, we housed S1PR2 mice in separate cages, one cage treated with tamoxifen and while the

other was not. There was no “leakiness” of the reporter in mice that were not treated with tamoxifen (Fig. S3A).

We next focused on S1PR2 expression among the GC B cells and the DP Ig+ MBC populations. As expected, nearly all of the GC B cells and DP Ig+ MBCs at day ≥50 expressed the S1PR2 fate reporter, demonstrating effective labeling. Unexpectedly however, we found that only half of the DP IgM+ MBCs expressed the S1PR2 fate reporter (Fig. 4 A). The heterogeneous S1PR2 expression on DP IgM+ MBCs was confounding because we anticipated that the cells were GC-dependent and would all be S1PR2+. Alternatively, if the cells were GC-independent, they would all be S1PR2-. Therefore, in order to test whether the DP IgM+ MBCs capable of rapidly forming secondary plasmablasts are GC-derived, we also rechallenged the mice and analyzed S1PR2 expression on the responding cells. While only half of the DP IgM+ MBCs expressed S1PR2, nearly all (~90%) of the secondary plasmablasts were S1PR2+ (Fig. 4B). To verify that these secondary plasmablasts were coming from previously labeled MBCs, we also infected mice that we did not treat with tamoxifen until secondary challenge and saw that none of the plasmablasts were labeled (Fig S3B). These data suggest that despite heterogeneity of SIPR2 labeling of the DP IgM+ population, MBCs that rapidly form antibody secreting cells are SIPR2 fate-mapped.

Somatically hypermutated DP IgM+ MBCs can form in the absence of both GCs and Tfh cells

Our previous results indicated that the DP memory B cells that respond to rechallenge are BCL6-dependent and express SIPR2 during the labeling period, suggesting GC-dependence. To test this hypothesis, we examined the generation of these cells in a GC-deficient environment, without genetically modifying the B cell lineage. Effector CD4+ T cells that do not express BCL6 do not form CXCR5+ T follicular helper (Tfh) cells, which interact with and differentiate B cells at the T-B border (*43*). We therefore tested whether BCL6 deletion in CD4+ T

was required for DP MBC formation *CD4-Cre*+ mice were crossed with *BCL6flx/flx* mice in order to generate mice with *T cell* intrinsic ablation of BCL6 (BCL6TKO), rather than the B cell specific ablation we had previously used.

To confirm that GCs did not develop in the BCL6TKO mice, we performed histology on spleens from WT and BCL6TKO mice at days 0 (i.e. naïve), 8 and 15-20 post-infection. We quantified GC structures based on IgD, CD35, CD3 and BCL6 staining. Non-GC clusters were defined as BCL6+ cells surrounded by IgD+ follicular B cells with the CD35+ network throughout. Mature GCs were defined as a cluster of BCL6+ cells surrounded by IgD+ follicular B cells with a polarized CD35+ network. In naïve mice, there were few non-GC clusters (Fig. S4A, B). Because the mice were not housed in a germ-free facility, these likely formed in response to environmental antigens. However, at day 8 post-infection, non-GC clusters were found in both WT and BCL6TKO spleens, and mature GCs had also started to develop in the WT mice but not the BCL6TKO mice (Fig. S4A, B). By days 15-20 post-infection the WT mice had increased mature GCs, yet these were not found in the BCL6TKO (Fig. S4A, B). These data demonstrate that as previously published, BCL6 expression within the T cell compartment is necessary for the development of mature GCs.

We next examined whether CD4+ Tfh cells were required for both IgM+ and IgG+ DP MBCs. By day 28 post-infection, there were far fewer MSP1-specific B cells in mice that lacked Tfh cells and specifically, the GC B cell population was abolished as expected (Fig. S4C, D). Moreover, 28 days after infection, the total number of MSP1-specific CD38+GL7- MBCs were comparable in the two experimental groups, yet the composition of the populations was strikingly different. Class-switched MBCs from BCL6TKO mice were severely diminished compared to WT mice. However, the IgM+ and IgD+ MBCs populations from BCL6TKO mice were comparable in percentage and number to those found in WT mice (Fig. 5A). We therefore concluded that while the majority of the swIg+ MBC population is dependent on Tfh cells and GCs, surprisingly the unswitched IgM+ MBCs are able to form in a Tfh cell-independent manner.

These findings raised the possibility that while the numbers of IgM+ MBCs were the same in the presence or absence of Tfh cells, perhaps we had removed key differentiation cues that altered the generation of DP somatically hypermutated cells. Further analyses of CD73 and CD80 expression revealed comparable levels of these molecules on IgM+ MBCs in the WT and Tfh-deficient environments, while there was a pronounced loss of DP swIg+ MBC in BCL6TKO mice compared to WT mice (Fig. 5B). We had previously shown that in WT mice, DP IgM+ MBCs expressed somatically hypermutated BCRs (Krishnamurty *et al.*, 2016). Therefore, we next sought to determine if the levels of somatic hypermutation among the DP IgM+ MBCs were also comparable in the presence or absence of Tfh cells. To that end, we performed single cell BCR sequencing of sorted MBCs from both groups of mice. We were unable to sort enough MSP1-specific swIg+ cells from the BCL6TKO mice to include in this analysis as very few were generated in the absence of Tfh cells (Fig. 5B, C). As expected, IgD+ cells from either WT or BCL6TKO mice had very low levels of CD73 and CD80 expression, and also very few mutations in their BCRs (Fig. 5B, C). However, mutational analyses of generated sequences revealed that MSP1-specific DP IgM+ MBCs from WT and Tfh cell-deficient mice had similar levels of somatic hypermutation (Fig. 5C), further demonstrating that this population of IgM+ MBCs can arise in the absence of CD4+ Tfh cells or GCs.

To address whether DP IgM+ MBCs can also develop independently of Tfh cells in other inflammatory settings or whether this phenotype was unique to *Plasmodium*, we examined the formation of LCMV glycoprotein (GP)-specific MBCs in WT and BCL6TKO mice infected with the Armstrong strain of LCMV (Fig S5A) and PE-specific MBCs in mice immunized with PE protein in adjuvant (Fig. S5B). As seen with *Plasmodium* infection, the total number of GP-specific or PE-specific IgD+ and DP IgM+ MBCs were not affected by the loss of the Tfh compartment whereas the DP swIg+ MBCs were severely diminished in both settings (Fig. S~~5~~A, B). Additionally, to validate that the presence of the CD4Cre recombinase (as opposed to deletion of BCL6) was not affecting our results, we

included Bcl6WT CD4Cre+ mice as controls rather than Bcl6flx/flx CD4Cre- mice. These experiments confirmed that the swIg+, but not the IgM+, DP MBCs are dependent Bcl6 expression in the T cell compartment (Fig. S5C). Together, these data demonstrate that while both DP IgM+ and DP swIg+ MBCs are somatically hypermutated, albeit to varying degrees, only the DP swIg+ MBCs require the presence of Tfh cells and GCs in order to undergo SHM. DP IgM+ memory B cells can undergo somatic hypermutation outside of the GC reaction.

The GC is not required for rapid secondary plasmablast formation

We had hypothesized that because the DP IgM+ MBCs that respond to secondary challenge expressed S1PR2, the DP IgM+ MBC population would be absent in mice lacking GCs. We were surprised that this population appeared to be intact in the BCL6TKO mice. However, it was possible that the population of DP IgM+ MBCs that are capable of rapidly forming secondary plasmablasts are GC-dependent and would be absent in the Tfh-deficient mice.

Our previous experiments had compared the ability of different MBC populations to respond to secondary challenge within individual mice, however genetic ablation of the Tfh compartment necessitated comparing populations of cells in different groups of mice. When we assessed parasitemia in WT and BCL6TKO we found that there were no significant differences in parasitemia through day 30 post-infection, consistent with previous results (Fig. S6A) (*44*). However, to ensure that the plasmablasts formed were induced by secondary infection rather than any sub-patent parasites that still remained in the blood at undetectable levels, we treated WT and BCL6TKO mice with atovaquone prior to rechallenge. At 3 days post-secondary challenge we examined secondary plasmablast formation. There was no significant difference between the ability of the WT and the BCL6TKO mice to mount a secondary IgM+ plasmablast response (Fig 6A, B), demonstrating the intact functionality of the Tfh-independent DP IgM+ MBCs. We also confirmed this phenotype using the PE immunization setting and saw similar results (Fig. S6B).

DISCUSSION

Several recent reports have identified transcriptional and epigenetic differences in MBC subsets (*10, 11*). These studies presented herein begin to elucidate the kinetics and developmental processes that govern the generation of these MBC populations during infection. Here, we have shown that–after infection with *Plasmodium*, BCL6 is upregulated in B cells prior to entry into the GC, findings that are consistent with several published studies using immunization strategies (*25, 29, 30*). BCL6 expression within B cells is T cell dependent (*29*), and is intrinsically required within B cells for the development of all DP MBC populations that form plasmablasts in response to a secondary challenge. Of interest, a subset of somatically hypermutated DP MBCs can be generated in GC-deficient mice. Thus, these data demonstrate that B cell expression of BCL6 is not limited to cells fated to enter a GC.

Rather, these results suggest that BCL6 has an essential function(s) in the development of MBC responses, independent of its role in GC formation. For example, BCL6 contains multiple DNA-binding domains that exert temporally and functionally distinct effects on the B cell response (*45, 46*). One possibility therefore is that in the absence of BCL6, which represses the DNA damage sensor ATR (*47*), B cells are not able to withstand DNA damage. As shown above, our data demonstrate that even though these cells develop independently of the GC, DP IgM+ MBCs still undergo SHM, which is associated with rapid proliferation and, by definition, damage to the DNA. It therefore follows that being able to withstand DNA damage would be essential to the survival of these cells.

It was quite striking that in our system ablation of the GC and the absence of Tfh cells did not prevent the development of somatically hypermutated DP IgM+ MBCs or the rapid secondary plasmablast response. The previous model for the role of the GC in MBC development suggested that only low affinity, unmutated DN MBCs could be generated independently of the GC; however, high affinity, mutated DP MBCs were dependent on GC establishment. Our data

provide evidence that GCs are only required for the majority of DP *class-switched* MBCs, whereas mutated DP MBCs that retain IgM expression bypass the GC during their development.

Similarly, the GC is often considered to be the sole location of somatic hypermutation of BCRs (*48*), yet in keeping with the work of others, the studies presented here demonstrate that somatic hypermutation can take place outside of the GC. For example, Shlomchik and colleagues have reported that somatic hypermutation can occur at the T zone-red pulp border (*49*), and somatically hypermutated swIg+ plasmablasts are formed in extrafollicular sites during infection with *Salmonella typhirmurium* or *Ehrlichia muris* (*50, 51*). Recent studies from the Jenkins laboratory have demonstrated that isotype-switched plasmablasts are able to form in the absence of T follicular helper cells (*52*). In our studies, we observed SHM in a subset of memory B cells in Tfh-deficient mice.

We therefore propose a new model in which a continuum of CD4+ T cell help defines functional MBC generation. IgD+ MBCs are not dependent on CD4+ T cell cognate interactions, BCL6 expression, or the GC. Classically defined somatically hypermutated class-switched MBCs do not arise when cognate interactions, intrinsic BCL6 expression, or the development of the GC is abrogated. However, an additional program occurs in a portion of cells that are T-dependent and BCL6 dependent yet that bypass the GC on their way to becoming MBCs. The cells derived from this program are bona fide MBCs that are somatically hypermutated and are able to rapidly respond after secondary antigen encounter. We were surprised that these cells also expressed S1PR2 as expression of this receptor is considered to be exclusive to the GC. However, several recent studies have brought this dogma into question. For example, a recent report using an NP-immunization has shown that S1PR2 expression on B cells can occur in a T-independent manner (*53*). Furthermore, studies from the Nussenzweig laboratory have identified a population of IgD- activated cells that express S1PR2 yet have not fully downregulated CD38 (i.e. within the activated

pre-GC compartment)(*23*). Similarly, in our studies we first detected S1PR2+ cells in the pre-GC gate at early timepoints (data not shown).

Despite these findings, the GC still serves a critical function in the generation of humoral immunity. Indeed, ablation of the GC leads to a severe reduction in class-switched memory B cells, LLPCs, and the inability to control parasite recrudescence (*44*). Nevertheless, these studies give us further insight into the intricacies of endogenous memory B cell development after infection and protein immunization and challenge current paradigms of MBC development. It will be important to consider these findings in different inflammatory contexts, such as designing novel vaccine strategies that are better able to generate the specific MBC subsets that are able to rapidly respond and are optimal for protection against subsequent infection.

Materials and Methods

Mice

C57BL/6 (CD45.2+), B6.SJL-Ptprc^{a} Pepc^{b}/BoyJ (CD45.1+), B6.Cg-Tg(Cd4-cre)1Cwi/BfluJ (CD4-Cre+), and B6.129S2-*Ciita*^{tm1Ccum}/J (MHCII$^{-/-}$) mice were purchased from The Jackson Laboratory. CD45.1+ mice were crossed to C57BL/6 (CD45.2+) mice to generate CD45.1+CD45.2+ mice. Mb1Cre+ mice were provided by Dr. Michael Reth (Max Planck Institute of Immunobiology and Epigenetics) and crossed to Bcl6flx/flx mice, provided by Dr. Alexander Dent (Indiana University), to generate MB1-Cre+Bcl6flx/flx mice. S1PR2-ERT2Cre+ mice were kindly provided by Tomohiro Kurasaki (Osaka University). CD4-Cre+ mice were crossed to Bcl6flx/flx mice to generate CD4-Cre+ Bcl6flx/flx mice. All experiments used sex-matched and age-matched mice that were maintained/bred under specific pathogen-free conditions at the University of Washington. All experiments were performed in accordance with the University of Washington Institutional Care and Use Committee guidelines.

Infections, drug treatment and parasitemia analysis

Plasmodium chabaudi chabaudi (AS) parasites were maintained as frozen blood stocks and passaged through donor mice. Primary mouse infections were initiated by intraperitoneal (i.p.) injection of $1x10^6$ iRBCs from donor mice. Secondary mouse infections were performed using a dose of $1x10^7$ iRBCs injected intravenously (i.v.). When indicated, mice were treated intraperitoneally with 14.4mg/kg atovaquone resuspended in DMSO (Sigma) on days 7-11. When indicated, mice were treated with tamoxifen in chow (Envigo) and/or intraperitoneal injection of 1mg tamoxifen (Sigma) in corn oil prior to infection and continuing through the duration of the experiment. Parasitemia was measured by flow cytometry by fixing a drop of blood with 0.025% glutaraldehyde and staining with Ter119 FITC, CD45 APC, Hoechst33342, and CD71 PE. For LCMV experiments, mice were infected intraperitoneally with 10^5 PFU of LCMV-Armstrong. For memory PE experiments, mice were injected at the base of the tail with 15ug PE in CFA. For secondary PE responses, previously immunized mice were given 60ug PE in CFA intraperitoneally (*54*).

Bone Marrow Chimeras

Bone marrow cells were collected from the tibia, femur, humerus, and sternum and labeled with anti-Thy1.2 (30-H12, eBioscience) and anti-NK1.1 (PK136, eBioscience). Cells were resuspended and incubated with low toxicity rabbit complement (Cedarlane Laboratories). After complement lysis, cells were washed with media containing 10% fetal calf serum. Recipient mice were lethally irradiated (1000 rads) and injected intravenously with $5x10^6$ total bone marrow cells with congenically disparate WT cells mixed with $MHCII^{-/-}$ or MB1-Cre+ Bcl6flx/flx cells mixed in equal portions and treated with antibiotic (Enrofloxacin)-treated water for 8 weeks. Prior to infection, chimerism was determined analyzing the ratio of CD45.1 and CD45.2 expression among B220+ cells. In order to adjust for differences in initial chimerism, this ratio was then applied to the calculations obtained after infection.

Tetramers

Purified recombinant His-tagged C-terminal MSP1 protein (amino acids 4960 to 5301) (*55*) was biotinylated and tetramerized with streptavidin-PE or streptavidin-APC (Prozyme), as previously described (*5*). LCMV Glycoprotein (GP) (provided by Dr. John Teijaro, Scripps Research Institute) was biotynylated and tetramerized with streptavidin-APC (Prozyme). Decoy reagent to exclude non-specific binding to the MSP1-PE tetramer was made by conjugating SA-PE to AF647 using an AF647 protein labeling kit (ThermoFisher), washing and removing any unbound AF647, and incubating with an excess of an irrelevant biotinylated His-tagged protein (*5, 56*). Decoy reagent to exclude non-specific binding to the MSP1-APC or GP-APC tetramer was made by conjugating SA-APC to DyLight 755 using a DyLight 755 antibody labeling kit (ThermoFisher), washing and removing any unbound DyLight 755, and incubating with an excess of an irrelevant biotinylated His-tagged protein.

Mouse Cell Enrichment and Flow Cytometry

Splenic single-cell suspensions were prepared by mashing spleens and passing through 100um Nitex mesh (Amazon.com). For B cell enrichment, cells were resuspended in 200uL in PBS containing 2% FBS and Fc block (2.4G2) and first incubated with Decoy tetramer at a concentration of 10nM at room temperature for 20 min. MSP1-PE tetramer or MSP1-APC tetramer was added at a concentration of 10nM and incubated on ice for 30 min. Cells were washed, incubated with anti-PE or anti-APC magnetic beads for 30 min on ice, and enriched for using magnetized LS columns (Miltenyi Biotec). All bound cells were stained with surface antibodies followed by fixation and intracellular antibody staining when needed (Table 1). Cell counts were determined using Accucheck cell counting beads. All cells were run on the LSRII or Symphony (BD) and analyzed using FlowJo software (Treestar).

Single cell BCR sequencing

Single naïve MSP1^{+} B cells, and IgD+, DP IgM+ and DP IgG+ MBCs were FACS sorted using an ARIAII into 96-well plates. cDNA was prepared using the Maxima First Strand cDNA Syntheis Kit (Thermo Fisher) and BCRs were amplified using the primers in Table 2. DNA products were purified with Exocnuclease and Alkaline Phosphatase (Thermo Fisher) and sequenced by Genewiz. Nucleotide sequences were analyzed using IgBlast to determine the number of mutations from the germline sequence.

Histology

Spleens were fixed in 4% PFA for 2 hours at 4°C, washed three times for 10 min in 1X PBS and sunk in 30% sucrose overnight before freezing–in OCT. 7µm cryosections were dried for 1 hour and rehydrated in 1X PBS with 1% BSA for 10 min. Sections were stained in antibody overnight at 4˚C, washed for 10min in 1X PBS with 1% BSA and stained in secondary antibody for 2 hours at room temperature. All stains were done in 1X PBS with 2% normal mouse serum (Jackson Immunoresearch), 2% normal rat serum (Jackson Immunoresearch) and 1% BSA. Antibodies used were anti-IgD ef450 (11-26c, eBioscience), anti-CD3 Alexa488 (17A2, BioLegend), anti-CD35 biotin (8C12, BD Pharmingen), anti-BCL6 Alexa647 (K112-91, BD Biosciences) and streptavidin Cy3 (Jackson Immunoresearch). Immunofluoresence microscopy images were captured with a Nikon Eclipse Ti microscope and analyzed with NIS-Elements AR.

Statistical Analysis

Two-tailed Student's *t* tests were applied to determine the statistical significance of the differences between individual groups. One way ANOVA was used to determine the statistical significance of the differences between multiple groups. A paired *t* test was applied to determine statistical significance within individual mixed bone marrow chimeras. All analyses were done with Prism (Graphpad)

software. The p-values were considered significant when $p < 0.05$ (*), $p < 0.01$ (**), and $p<0.001$ (***).

List of Supplementary Materials

Figure S1. MHCII:peptide cognate interactions are required for MSP1-specific B cell responses

Figure S2. Heterogeneous B cells populations are dependent on intrinsic expression of BCL6**.**

Figure S3. Fidelity of S1PR2 reporter.

Figure S4. Mature GCs do not form in BCL6TKO mice in response to P. chabaudi infection**.**

Figure S5. Analysis of antigen-specific B cell responses in WT and BCL6TKO, and CD4Cre+ mice

Figure S6. Additional data for WT and BCL6TKO mice

Table1. List of antibodies used

Table 2. BCR sequencing primers

References

1. S. A. Plotkin, Correlates of protection induced by vaccination. *Clin Vaccine Immunol* **17**, 1055-1065 (2010).
2. T. Inoue, T. Kurosaki, Memory B cells. *Nat Rev Immunol* **24**, 5-17 (2024).
3. M. Akkaya, K. Kwak, S. K. Pierce, B cell memory: building two walls of protection against pathogens. *Nat Rev Immunol* **20**, 229-238 (2020).
4. G. Harms Pritchard, M. Pepper, Memory B cell heterogeneity: Remembrance of things past. *J Leukoc Biol* **103**, 269-274 (2018).
5. A. T. Krishnamurty *et al.*, Somatically Hypermutated Plasmodium-Specific IgM(+) Memory B Cells Are Rapid, Plastic, Early Responders upon Malaria Rechallenge. *Immunity* **45**, 402-414 (2016).
6. M. Seifert *et al.*, Functional capacities of human IgM memory B cells in early inflammatory responses and secondary germinal center reactions. *Proc Natl Acad Sci U S A* **112**, E546-555 (2015).
7. F. J. Weisel, G. V. Zuccarino-Catania, M. Chikina, M. J. Shlomchik, A Temporal Switch in the Germinal Center Determines Differential Output of Memory B and Plasma Cells. *Immunity* **44**, 116-130 (2016).

8. J. L. Yates, R. Racine, K. M. McBride, G. M. Winslow, T cell-dependent IgM memory B cells generated during bacterial infection are required for IgG responses to antigen challenge. *J Immunol* **191**, 1240-1249 (2013).
9. G. V. Zuccarino-Catania *et al.*, CD80 and PD-L2 define functionally distinct memory B cell subsets that are independent of antibody isotype. *Nat Immunol* **15**, 631-637 (2014).
10. M. J. Price, C. D. Scharer, A. K. Kania, T. D. Randall, J. M. Boss, Conserved Epigenetic Programming and Enhanced Heme Metabolism Drive Memory B Cell Reactivation. *J Immunol* **206**, 1493-1504 (2021).
11. D. Callahan *et al.*, Memory B cell subsets have divergent developmental origins that are coupled to distinct imprinted epigenetic states. *Nat Immunol*, (2024).
12. I. Dogan *et al.*, Multiple layers of B cell memory with different effector functions. *Nat Immunol* **10**, 1292-1299 (2009).
13. L. Mesin *et al.*, Restricted Clonality and Limited Germinal Center Reentry Characterize Memory B Cell Reactivation by Boosting. *Cell* **180**, 92-106.e111 (2020).
14. S. Crotty, A brief history of T cell help to B cells. *Nat Rev Immunol* **15**, 185-189 (2015).
15. I. Papa, C. G. Vinuesa, Synaptic Interactions in Germinal Centers. *Front Immunol* **9**, 1858 (2018).
16. T. Kaji *et al.*, Distinct cellular pathways select germline-encoded and somatically mutated antibodies into immunological memory. *J Exp Med* **209**, 2079-2097 (2012).
17. A. W. Y. Lau *et al.*, BAFFR controls early memory B cell responses but is dispensable for germinal center function. *J Exp Med* **218**, (2021).
18. T. Takemori, T. Kaji, Y. Takahashi, M. Shimoda, K. Rajewsky, Generation of memory B cells inside and outside germinal centers. *Eur J Immunol* **44**, 1258-1264 (2014).
19. J. J. Taylor, K. A. Pape, M. K. Jenkins, A germinal center-independent pathway generates unswitched memory B cells early in the primary response. *J Exp Med* **209**, 597-606 (2012).
20. J. J. Taylor, M. K. Jenkins, K. A. Pape, Heterogeneity in the differentiation and function of memory B cells. *Trends Immunol* **33**, 590-597 (2012).
21. H. Toyama *et al.*, Memory B cells without somatic hypermutation are generated from Bcl6-deficient B cells. *Immunity* **17**, 329-339 (2002).
22. V. Glaros *et al.*, Limited access to antigen drives generation of early B cell memory while restraining the plasmablast response. *Immunity* **54**, 2005-2023.e2010 (2021).
23. C. Viant *et al.*, Germinal center-dependent and -independent memory B cells produced throughout the immune response. *J Exp Med* **218**, (2021).
24. R. L. Reinhardt, H. E. Liang, R. M. Locksley, Cytokine-secreting follicular T cells shape the antibody repertoire. *Nat Immunol* **10**, 385-393 (2009).

25. S. M. Kerfoot *et al.*, Germinal center B cell and T follicular helper cell development initiates in the interfollicular zone. *Immunity* **34**, 947-960 (2011).
26. H. Qi, J. L. Cannons, F. Klauschen, P. L. Schwartzberg, R. N. Germain, SAP-controlled T-B cell interactions underlie germinal centre formation. *Nature* **455**, 764-769 (2008).
27. P. Garside *et al.*, Visualization of specific B and T lymphocyte interactions in the lymph node. *Science* **281**, 96-99 (1998).
28. T. A. Schwickert *et al.*, A dynamic T cell-limited checkpoint regulates affinity-dependent B cell entry into the germinal center. *J Exp Med* **208**, 1243-1252 (2011).
29. M. Kitano *et al.*, Bcl6 protein expression shapes pre-germinal center B cell dynamics and follicular helper T cell heterogeneity. *Immunity* **34**, 961-972 (2011).
30. T. T. Zhang *et al.*, Germinal center B cell development has distinctly regulated stages completed by disengagement from T cell help. *Elife* **6**, (2017).
31. H. Niu, G. Cattoretti, R. Dalla-Favera, BCL6 controls the expression of the B7-1/CD80 costimulatory receptor in germinal center B cells. *J Exp Med* **198**, 211-221 (2003).
32. A. L. Dent, A. L. Shaffer, X. Yu, D. Allman, L. M. Staudt, Control of inflammation, cytokine expression, and germinal center formation by BCL-6. *Science* **276**, 589-592 (1997).
33. T. Fukuda *et al.*, Disruption of the Bcl6 gene results in an impaired germinal center formation. *J Exp Med* **186**, 439-448 (1997).
34. B. H. Ye *et al.*, The BCL-6 proto-oncogene controls germinal-centre formation and Th2-type inflammation. *Nat Genet* **16**, 161-170 (1997).
35. E. Hobeika *et al.*, Testing gene function early in the B cell lineage in mb1-cre mice. *Proc Natl Acad Sci U S A* **103**, 13789-13794 (2006).
36. K. Hollister *et al.*, Insights into the role of Bcl6 in follicular Th cells using a new conditional mutant mouse model. *J Immunol* **191**, 3705-3711 (2013).
37. C. Peng *et al.*, BCL6-Mediated Silencing of PD-1 Ligands in Germinal Center B Cells Maintains Follicular T Cell Population. *J Immunol* **202**, 704-713 (2019).
38. U. Klein, R. Dalla-Favera, Germinal centres: role in B-cell physiology and malignancy. *Nat Rev Immunol* **8**, 22-33 (2008).
39. J. P. Pereira, L. M. Kelly, Y. Xu, J. G. Cyster, EBI2 mediates B cell segregation between the outer and centre follicle. *Nature* **460**, 1122-1126 (2009).
40. J. A. Green, J. G. Cyster, S1PR2 links germinal center confinement and growth regulation. *Immunol Rev* **247**, 36-51 (2012).
41. R. Shinnakasu *et al.*, Regulated selection of germinal-center cells into the memory B cell compartment. *Nat Immunol* **17**, 861-869 (2016).
42. C. Viant *et al.*, Antibody Affinity Shapes the Choice between Memory and Germinal Center B Cell Fates. *Cell* **183**, 1298-1311.e1211 (2020).

43. C. G. Vinuesa, M. A. Linterman, D. Yu, I. C. MacLennan, Follicular Helper T Cells. *Annu Rev Immunol* **34**, 335-368 (2016).
44. D. Pérez-Mazliah *et al.*, Follicular Helper T Cells are Essential for the Elimination of Plasmodium Infection. *EBioMedicine* **24**, 216-230 (2017).
45. C. Huang, K. Hatzi, A. Melnick, Lineage-specific functions of Bcl-6 in immunity and inflammation are mediated by distinct biochemical mechanisms. *Nat Immunol* **14**, 380-388 (2013).
46. C. Huang *et al.*, The BCL6 RD2 domain governs commitment of activated B cells to form germinal centers. *Cell Rep* **8**, 1497-1508 (2014).
47. S. M. Ranuncolo *et al.*, Bcl-6 mediates the germinal center B cell phenotype and lymphomagenesis through transcriptional repression of the DNA-damage sensor ATR. *Nat Immunol* **8**, 705-714 (2007).
48. N. S. De Silva, U. Klein, Dynamics of B cells in germinal centres. *Nat Rev Immunol* **15**, 137-148 (2015).
49. J. William, C. Euler, S. Christensen, M. J. Shlomchik, Evolution of autoantibody responses via somatic hypermutation outside of germinal centers. *Science* **297**, 2066-2070 (2002).
50. R. Di Niro *et al.*, Salmonella Infection Drives Promiscuous B Cell Activation Followed by Extrafollicular Affinity Maturation. *Immunity* **43**, 120-131 (2015).
51. N. Trivedi *et al.*, Liver Is a Generative Site for the B Cell Response to Ehrlichia muris. *Immunity* **51**, 1088-1101.e1085 (2019).
52. J. A. Kotov, M. K. Jenkins, Cutting Edge: T Cell-Dependent Plasmablasts Form in the Absence of Single Differentiated CD4. *J Immunol* **202**, 401-405 (2019).
53. X. Liu, Y. Zhao, H. Qi, T-independent antigen induces humoral memory through germinal centers. *J Exp Med* **219**, (2022).
54. K. A. Pape, J. J. Taylor, R. W. Maul, P. J. Gearhart, M. K. Jenkins, Different B cell populations mediate early and late memory during an endogenous immune response. *Science* **331**, 1203-1207 (2011).
55. F. M. Ndungu *et al.*, Functional memory B cells and long-lived plasma cells are generated after a single Plasmodium chabaudi infection in mice. *PLoS Pathog* **5**, e1000690 (2009).
56. J. J. Taylor *et al.*, Deletion and anergy of polyclonal B cells specific for ubiquitous membrane-bound self-antigen. *J Exp Med* **209**, 2065-2077 (2012).

Acknowledgements: Author contributions**:** GHP conceptualized, performed and analyzed experiments, prepared figures, wrote and edited the manuscript, ATK conceptualized, performed and analyzed experiments, prepared figures, and

edited the manuscript, LR performed and analyzed experiments and prepared figures, CM performed experiments, MP conceptualized and analyzed data from experiments and wrote and edited the manuscript. Funding**:** MP is supported by NIH RO1 A1-118803 and the Burroughs Wellcome Fund. GHP is supported by NIH R21 AI-166022-02. The authors would like to thank Brian Hondowicz, Chris Thouvenel, and Brian Johnson for technical assistance. We would also like to thank Dr. Michael Reth (Max Planck Institute of Immunobiology and Epigenetics) for providing the Mb1Cre+ mice, Dr. Alexander Dent (Indiana University), for providing the Bcl6flx/flx mice, Dr. Tomohiro Kurosaki (Osaka University) for providing the S1PR2-ERT2cre mice, and Dr. John Teijaro (Scripps Research Institute) for providing the LCMV GP protein.

FIGURE LEGENDS

Figure 1. Cognate T cell interactions are required for the generation of IgM+ and swIg+ MBCs. Chimeras were made using congenically disparate WT (CD45.1+) and MHCII-/- (CD45.2+) bone marrow mixed in equal proportions. After ≥ 8 weeks reconstitution, mice were infected with *P. chabaudi* and total MSP1-specific B cell responses (A) and MSP1-specific memory B cell responses (B) were assessed at the indicated timepoints. At ≥100 days post-infection, memory B cells were subsetted into IgD+, IgM+, and swIg+ isotypes (C). IgD+, IgM+ and swIg+ MBCs were examined for CD73 expression (D). Data at each timepoint are pooled from 2 individual experiments with 3-4 mice in each experiment

Figure 2. Kinetics of BCL6 expression in B cells. WT mice were infected with *P. chabaudi* and MSP1-specific B cell responses were assessed at the indicated timepoints. Gating strategy and quantification of BCL6+ cells (A,B). Gating strategy for IgD and BCL6 expression (C). Gating strategy and quantification of IgM+ and swIg+ BCL6+ cells (D). Gating strategy and quantification of CD80 expressing cells (E,F). Data are pooled from 9 independent experiments with 10-31 mice per timepoint.

Figure 3. B cell intrinsic expression of BCL6 is required for IgM+ and swIg+ MBCs.

Chimeras were made using congenically disparate WT (CD45.1+) and BCL6BKO (*Mb1Cre+Bcl6flx/flx*) (CD45.2+) bone marrow mixed in equal proportions. After ≥ 8 weeks reconstitution, mice were infected with *P. chabaudi* and MSP1-specific B cell responses were assessed at memory timepoints ≥44 days post-infection (A,B). MSP1+ MBCs were subsetted into IgD+, IgM+, and swIg+ isotypes (A), and CD73 and CD80 expression was assessed (B). Data are pooled from 2-4 individual experiments with 1-2 mice each. At memory timepoints (≥44 days post-infection), mice were either unchallenged (memory) or rechallenged intravenously with $1x10^7$

iRBCs and responses were analyzed by B220 and CD138 expression 3 days later (C). Data are pooled from 3 experiments with 1-3 mice per group in each experiment.

Figure 4. S1PR2 expression on B cell subsets. $Tdtomato^{flox}$S1PR2-ERT2Cre mice and control $Tdtomato^{flox}$ mice were administered tamoxifen and

subsequently infected with *P. chabaudi*. Tamoxifen administration was continued through the duration of the experiment. Gating strategy and quantification of GC B cells and DP IgM+ and swIg+ MBCs (A). Data are pooled from 4 independent experiments with 1-2 mice each. Tdtomato^{flox}S1PR2-ERT2Cre memory mice ≥ 50 days post-infection) were rechallenged with *P. chabaudi* and S1PR2 expression was assessed on the secondary plasmablasts 3 days later (B). Data are pooled from 5 independent experiments with 1-2 mice each.

Figure 5. Tfh cells are required for DP swIg+ MBCs but not DP IgM+ MBCs. WT and BCL6TKO mice were infected with *P. chabaudi.* At 28 days post-infection, MSP1-specific MBC responses were quantified and subsetted into IgD+, IgM+, and swIg+ isotypes (A), and CD73 and CD80 expression was assessed on these cells (B). Data are pooled from 3 individual experiments with 2-4 mice in each group. MSP1-specific B cells from 2 naïve mice and IgD+, DP IgM+, and DP swIg+ MBCs from 2 memory WT and 2 memory BCL6TKO mice were single-cell sorted and BCR heavy chains were sequenced and analyzed for the number of mutations compared to germline sequences (C).

Figure 6. Tfh cells are not required for rapid secondary plasmablast formation. WT and BCL6TKO mice were infected with *P. chabaudi* and treated with atovaquone daily for 5 days starting at day 7 post infection. At ≥28 days post infection, mice were rechallenged with *P. chabaudi* and the plasmablast response was quantified 3 days later (A). Proportion of IgM on the secondary plasmablast population was quantified (B).

Fig. 1.

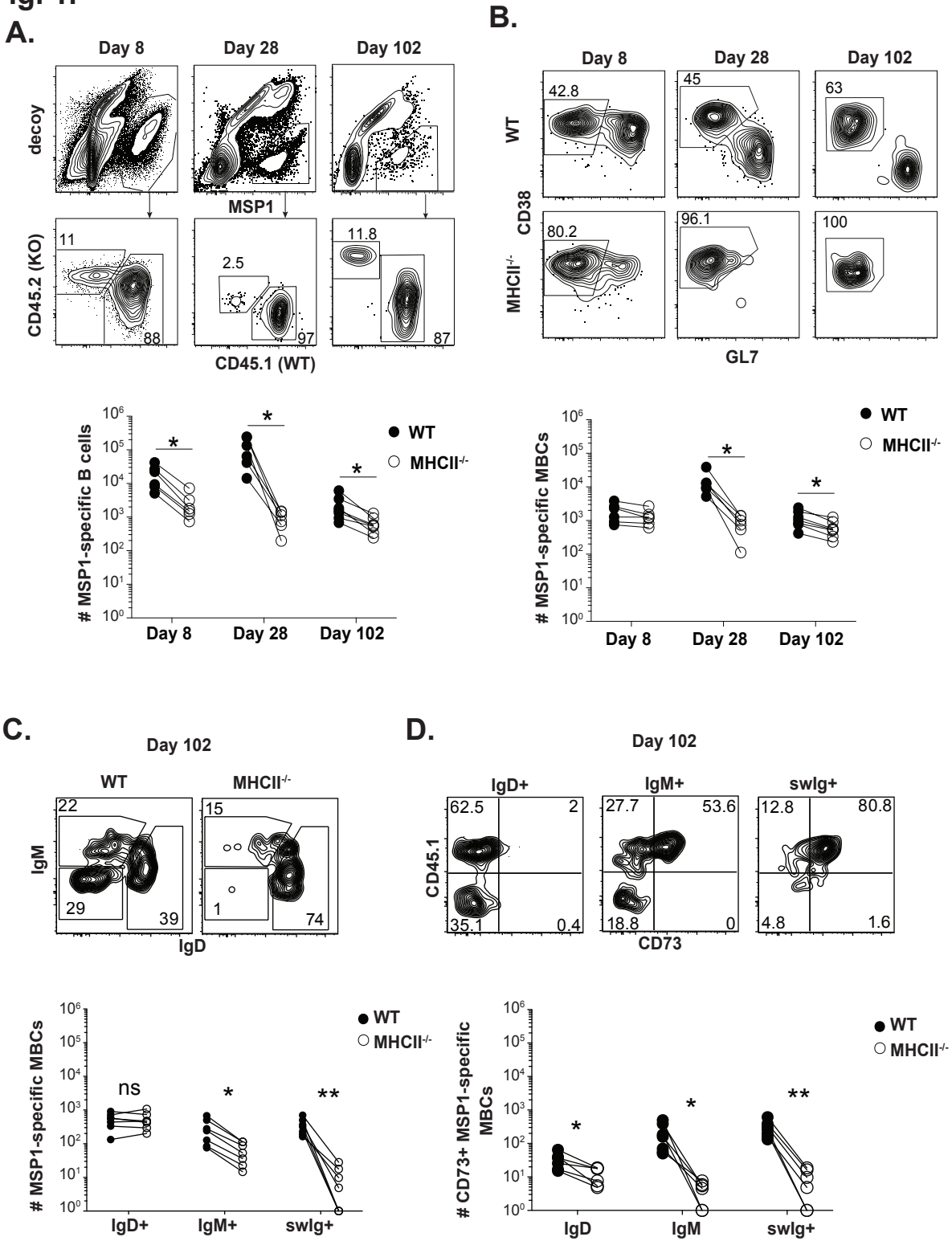
A.
Day 8
Day 28
Day 102
decoy
MSP1
CD45.2 (KO)
CD45.1 (WT)
11
88
2.5
97
11.8
87
B.
Day 8
Day 28
Day 102
WT
MHCII-/-
CD38
GL7
42.8
45
63
80.2
96.1
100
MSP1-specific B cells
MSP1-specific MBCs
WT
MHCII-/-
Day 8
Day 28
Day 102
C.
Day 102
WT
MHCII-/-
IgM
IgD
22
29
39
15
1
74
MSP1-specific MBCs
ns
IgD+
IgM+
swIg+
D.
Day 102
IgD+
IgM+
swIg+
CD45.1
CD73
62.5
2
35.1
0.4
27.7
53.6
18.8
0
12.8
80.8
4.8
1.6
CD73+ MSP1-specific MBCs
IgD
IgM
swIg+

Fig. 2.

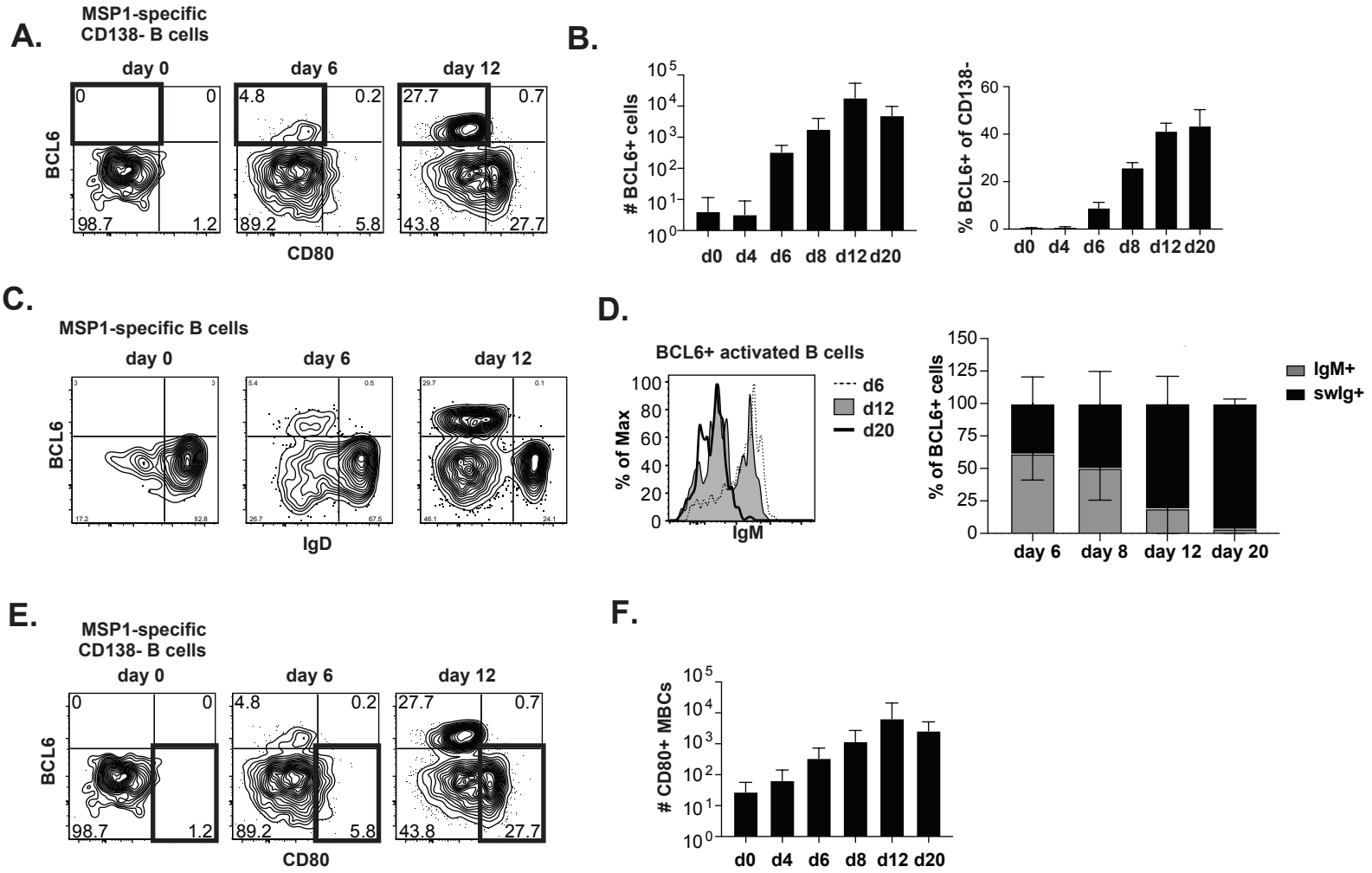
A.
MSP1-specific
CD138- B cells
day 0
day 6
day 12
BCL6
CD80
0
0
98.7
1.2
4.8
0.2
89.2
5.8
27.7
0.7
43.8
27.7
B.
BCL6+ cells
% BCL6+ of CD138-
d0 d4 d6 d8 d12 d20
C.
MSP1-specific B cells
day 0
day 6
day 12
BCL6
IgD
D.
BCL6+ activated B cells
% of Max
IgM
d6
d12
d20
% of BCL6+ cells
IgM+
swIg+
day 6 day 8 day 12 day 20
E.
MSP1-specific
CD138- B cells
day 0
day 6
day 12
BCL6
CD80
F.
CD80+ MBCs
d0 d4 d6 d8 d12 d20

Fig. 3.

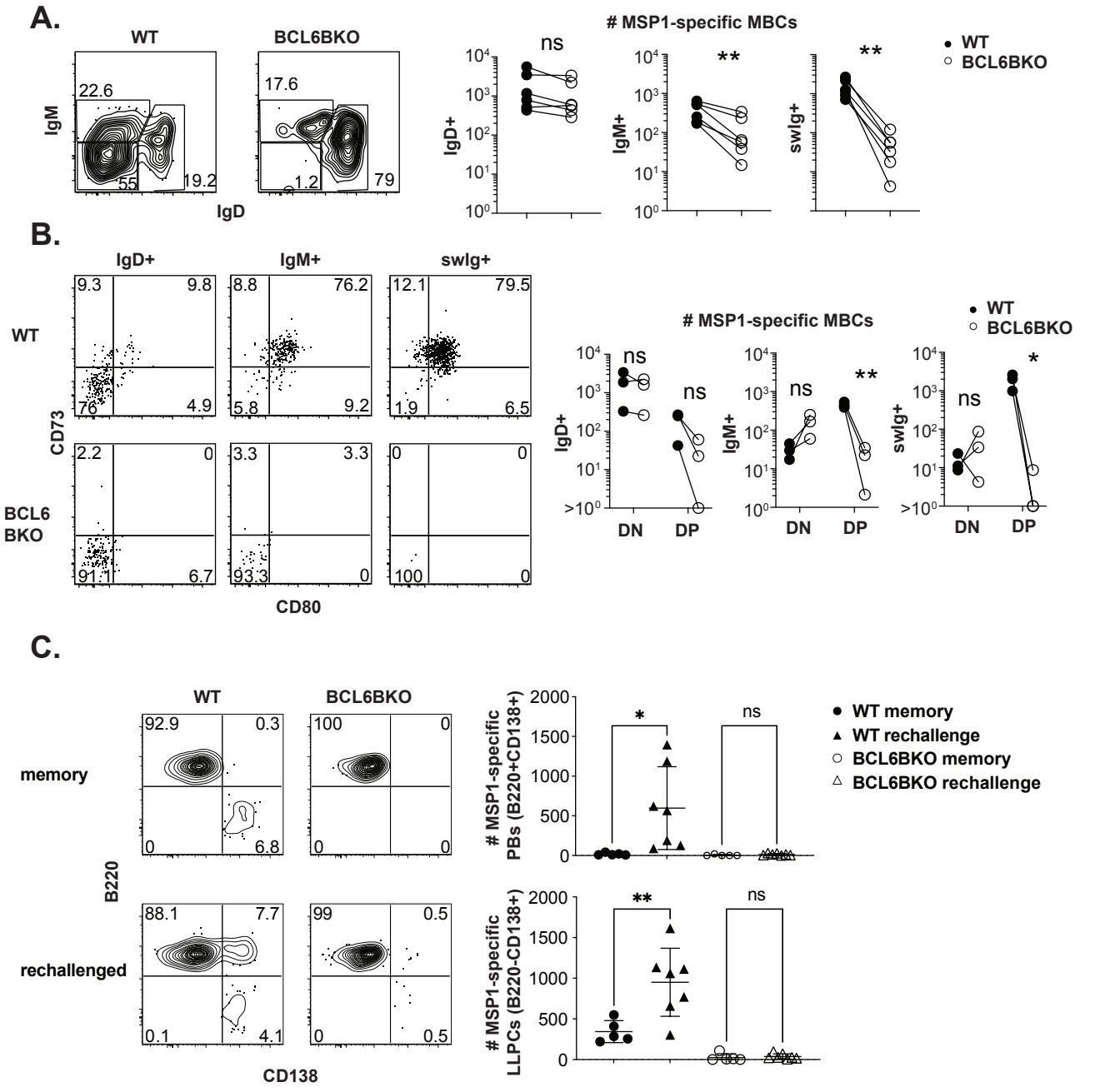
A.
WT
BCL6BKO
IgM
IgD
22.6
55
19.2
17.6
1.2
79
MSP1-specific MBCs
ns
**
**
IgD+
IgM+
swIg+
WT
BCL6BKO
B.
IgD+
IgM+
swIg+
WT
BCL6 BKO
CD73
CD80
9.3
9.8
76
4.9
8.8
76.2
5.8
9.2
12.1
79.5
1.9
6.5
2.2
0
91.1
6.7
3.3
3.3
93.3
0
0
0
100
0
MSP1-specific MBCs
WT
BCL6BKO
ns
ns
ns
**
ns
*
IgD+
IgM+
swIg+
DN
DP
C.
WT
BCL6BKO
memory
rechallenged
B220
CD138
92.9
0.3
0
6.8
100
0
0
0
88.1
7.7
0.1
4.1
99
0.5
0
0.5
MSP1-specific PBs (B220+CD138+)
MSP1-specific LLPCs (B220-CD138+)
*
ns
**
ns
WT memory
WT rechallenge
BCL6BKO memory
BCL6BKO rechallenge

Fig. 4.

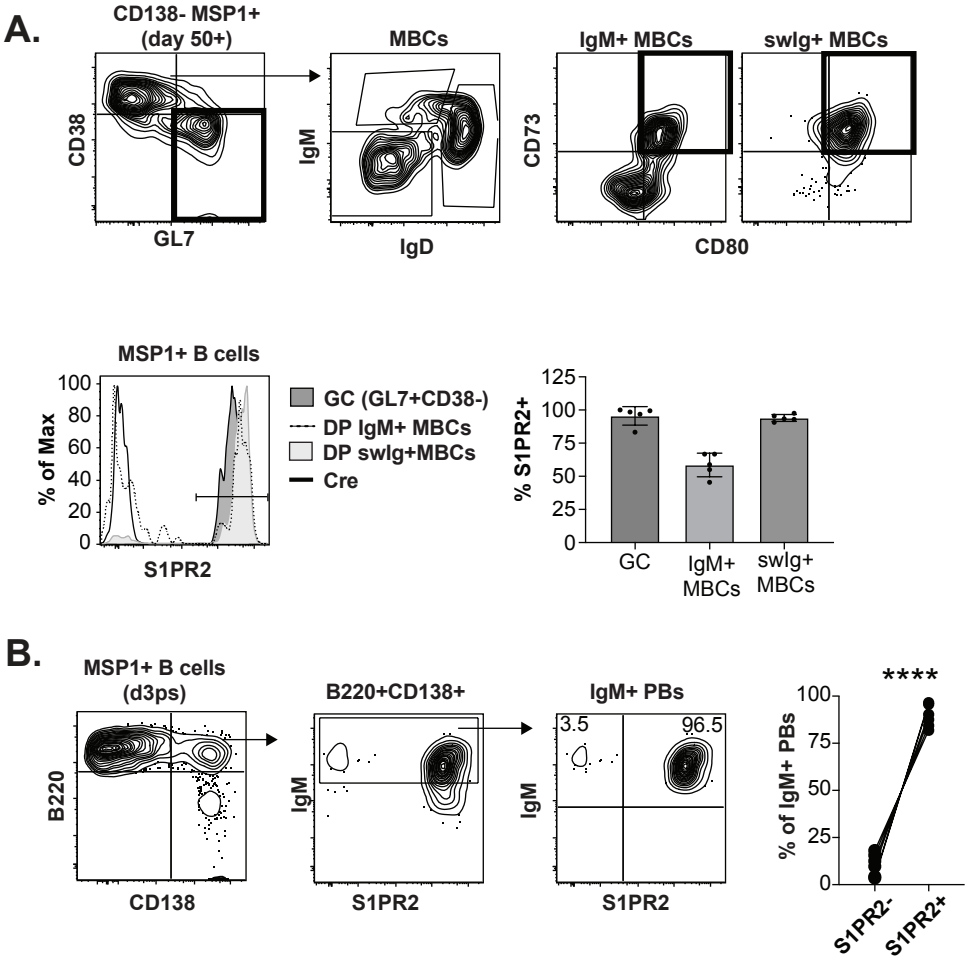
A.
CD138- MSP1+
(day 50+)
CD38
GL7
MBCs
IgM
IgD
IgM+ MBCs
swIg+ MBCs
CD73
CD80
MSP1+ B cells
% of Max
S1PR2
GC (GL7+CD38-)
DP IgM+ MBCs
DP swIg+MBCs
Cre
% S1PR2+
GC
IgM+ MBCs
swIg+ MBCs
B.
MSP1+ B cells
(d3ps)
B220
CD138
B220+CD138+
IgM
S1PR2
IgM+ PBs
3.5
96.5
IgM
S1PR2
****
% of IgM+ PBs
S1PR2-
S1PR2+

Fig. 5.

A.

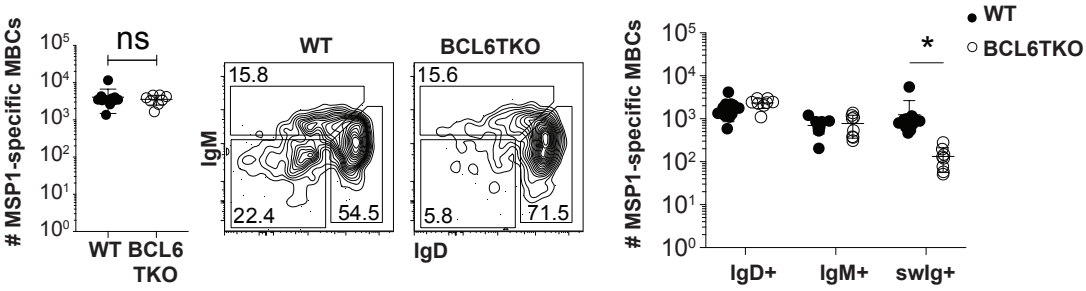
ns
MSP1-specific MBCs
WT BCL6 TKO
WT
BCL6TKO
15.8
22.4
54.5
15.6
5.8
71.5
IgM
IgD
*
WT
BCL6TKO
IgD+
IgM+
swIg+

B.

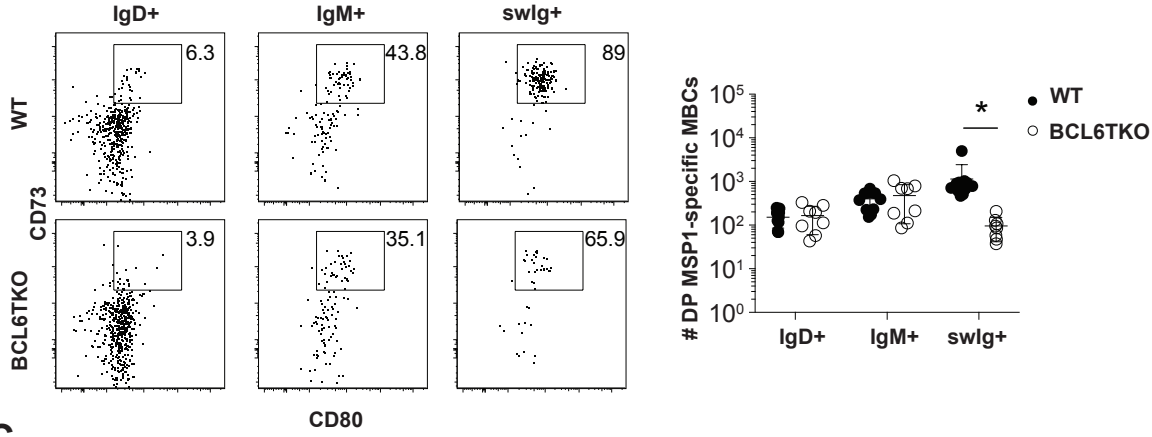
IgD+
IgM+
swIg+
WT
BCL6TKO
CD73
CD80
6.3
43.8
89
3.9
35.1
65.9
DP MSP1-specific MBCs
*
WT
BCL6TKO
IgD+
IgM+
swIg+

C.

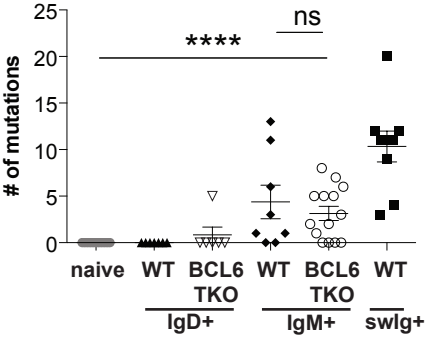
# of mutations
****
ns
naive
WT
BCL6 TKO
WT
BCL6 TKO
WT
IgD+
IgM+
swIg+

Fig. 6

A.

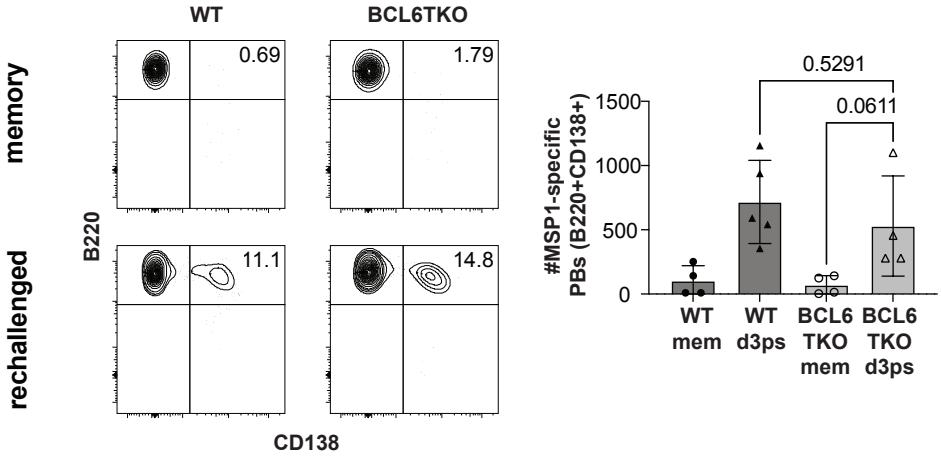
WT
BCL6TKO
memory
rechallenged
B220
CD138
0.69
1.79
11.1
14.8
#MSP1-specific PBs (B220+CD138+)
1500
1000
500
0
0.5291
0.0611
WT mem
WT d3ps
BCL6 TKO mem
BCL6 TKO d3ps

B.

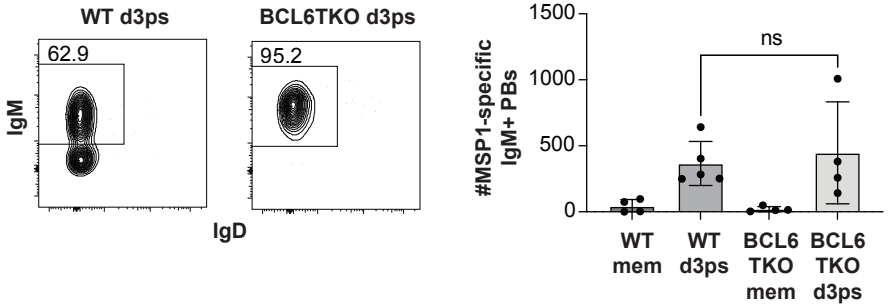
WT d3ps
BCL6TKO d3ps
IgM
IgD
62.9
95.2
#MSP1-specific IgM+ PBs
1500
1000
500
0
ns
WT mem
WT d3ps
BCL6 TKO mem
BCL6 TKO d3ps